

Upper limits on the diffuse supernova neutrino flux from the SuperKamiokande data

Cecilia Lunardini

Arizona State University, Tempe, AZ 85287-1504

*RIKEN BNL Research Center, Brookhaven National Laboratory, Upton, NY
11973*

Orlando L. G. Peres

Instituto de Física Gleb Wataghin - UNICAMP, 13083-970 Campinas SP, Brazil

Abstract

We analyze the 1496 days of SuperKamiokande data to put limits on the ν_e , $\bar{\nu}_e$, $\nu_\mu + \nu_\tau$ and $\bar{\nu}_\mu + \bar{\nu}_\tau$ components of the diffuse flux of supernova neutrinos, in different energy intervals and for different neutrino energy spectra. By considering the presence of only one component at a time, we find the following bounds at 90% C.L. and for neutrino energy $E > 19.3$ MeV: $\Phi_{\nu_e} < 73.3 - 154 \text{ cm}^{-2}\text{s}^{-1}$, $\Phi_{\bar{\nu}_e} < 1.4 - 1.9 \text{ cm}^{-2}\text{s}^{-1}$, $\Phi_{\nu_\mu + \nu_\tau} < (1.0 - 1.4) \cdot 10^3 \text{ cm}^{-2}\text{s}^{-1}$ and $\Phi_{\bar{\nu}_\mu + \bar{\nu}_\tau} < (1.3 - 1.8) \cdot 10^3 \text{ cm}^{-2}\text{s}^{-1}$, where the intervals account for varying the neutrino spectrum. In the interval $E = 22.9 - 36.9$ MeV, we find $\Phi_{\nu_e} < 39 - 54 \text{ cm}^{-2}\text{s}^{-1}$, which improves on the existing limit from SNO in the same energy window. Our results for $\nu_\mu + \nu_\tau$ and $\bar{\nu}_\mu + \bar{\nu}_\tau$ improve by about four orders of magnitude over the previous best constraints from LSD.

Key words: Neutrinos; Core Collapse Supernovae; Diffuse Cosmic Neutrino Fluxes

1 Introduction

The search for the diffuse flux of neutrinos from all supernovae represents a new frontier of neutrino astrophysics. Just like ultra-high energy neutrinos, the diffuse supernova neutrinos originate, for a good part, at cosmological

Email addresses: Cecilia.Lunardini@asu.edu (Cecilia Lunardini), orlando@ifi.unicamp.br (Orlando L. G. Peres).

distances. Therefore, they could give unique insights into the history of the universe, and specifically into the cosmological evolutions of the supernova rate and of the star formation rate, the physics of the first stars, etc.. This possibility, to do cosmology with neutrino data, is new. In addition to this, the diffuse flux will be a new test of the physics of core collapse supernovae and of neutrino propagation inside them, which will be especially important if a galactic supernova, a very rare event, does not occur in the next ten years or so.

Until now, the searches for the diffuse supernova neutrino flux (DSN ν F) have turned out negative, and upper limits were put. The strongest limit comes from the dominant detection mode – inverse beta decay, $\bar{\nu}_e + p \rightarrow n + e^+$ – in the largest water Cerenkov detector available, SuperKamiokande (SK), above the threshold of 19.3 MeV of neutrino energy [1]. The limit on the $\bar{\nu}_e$ component of the flux reads:

$$\Phi_{\bar{\nu}_e}(E > 19.3 \text{ MeV}) < 1.2 \text{ cm}^{-2}\text{s}^{-1} \quad \text{at } 90\% \text{C.L.} , \quad (1)$$

and is valid for certain energy spectra of the neutrino flux. This limit approaches the theoretical predictions [2,3,4,5,6,7,8,9,10,11,12,13,14,15,16], thus arising the expectation that the DSN ν F may be seen in the near future, and triggering several theoretical studies on the subject (see e.g. the review [17] and references therein).

Bounds on other neutrino species in the DSN ν F are weaker than the $\bar{\nu}_e$ limit (1), due to the fact that inverse beta decay largely dominates over other detection processes in water, and that non-water detectors have smaller volumes than SK.

Some attention has been devoted to the ν_e component of the DSN ν F. The strongest bound on this is indirect [18]:

$$\Phi_{\nu_e}(E > 19.3 \text{ MeV}) < 5.5 \text{ cm}^{-2}\text{s}^{-1} \quad \text{at } \sim 98\% \text{C.L.} . \quad (2)$$

It is found by converting the SK limit on $\bar{\nu}_e$, eq. (1), into a result for ν_e , using neutrino oscillations and the strong similarity between the fluxes of muon and tau neutrinos and antineutrinos produced inside a supernova.

Among the direct limits on ν_e , the strongest is from the search for charged current (CC) scattering on deuterium ($\nu_e + d \rightarrow p + p + e^-$) at the Sudbury Neutrino Observatory (SNO), in the interval 22.9 – 36.9 MeV of neutrino energy [19]. The result is:

$$\Phi_{\nu_e}(22.9 < E/\text{MeV} < 36.9) < 61 - 93 \text{ cm}^{-2}\text{s}^{-1} \quad \text{at } 90\% \text{C.L.} , \quad (3)$$

depending on the neutrino energy spectrum.

The old bounds from LSD [20] are still the best for the non-electron components of the flux, $\nu_\mu + \nu_\tau$ (ν_x from now on) and $\bar{\nu}_\mu + \bar{\nu}_\tau$ ($\bar{\nu}_x$ from now on). They are obtained from searches of neutrino scattering on ^{12}C , and read:

$$\begin{aligned}\Phi_{\nu_x}(20 < E/\text{MeV} < 100) &< 3 \cdot 10^7 \text{ cm}^{-2}\text{s}^{-1} \quad \text{at 90\%C.L.} , \\ \Phi_{\bar{\nu}_x}(20 < E/\text{MeV} < 100) &< 3.3 \cdot 10^7 \text{ cm}^{-2}\text{s}^{-1} \quad \text{at 90\%C.L.} .\end{aligned}\quad (4)$$

In this paper we examine the SK data published in [1] and use them to put limits on all the distinct components of the DSN ν F: ν_e , $\bar{\nu}_e$, ν_x and $\bar{\nu}_x$.

For $\bar{\nu}_e$, we elaborate on the result (1), by generalizing the SK analysis to a wider range of neutrino spectra, motivated by the recent progress in the theory. Our result is that the bound (1) could change by up to $\sim 50\%$ depending on the neutrino spectrum.

For the ν_e , ν_x and $\bar{\nu}_x$ components of the flux, the idea is to look for events due to CC scattering of ν_e on oxygen, or due to elastic scattering on electrons of neutrinos and antineutrinos of any flavor, on top of the irremovable background. These events are indistinguishable from inverse beta decay, since they have the same signature in the detector, the Cerenkov light produced by the outgoing lepton. One expects that, with respect to the SNO search for ν_e , the larger SK volume could overcompensate the disadvantage of the smaller detection cross section, resulting in a competitive limit. A similar argument makes us expect a strong improvement on the LSD limits for the non-electron species, Eq. (4). Our numerical analysis confirms these intuitions.

The paper is structured as follows. In sec. 2 we give generalities on the DSN ν F and discuss its energy spectrum. Sec. 3 is a review of the SK data and of our analysis of them. In sec. 4 we present results. Summary and discussion follow in sec. 5.

2 Generalities

2.1 Neutrinos from core collapse and the diffuse flux

A core collapse supernova is an extremely powerful neutrino source, releasing about $3 \cdot 10^{53}$ ergs of energy within ~ 10 seconds in neutrinos and antineutrinos of all flavors in similar amounts. The energy spectrum of these neutrinos at the production point in the star is roughly thermal, and can be described by a power law times an exponential [21]. The neutrinos have average energies in the range of 10 – 20 MeV, with the muon and tau species having harder

spectrum than the electron ones due to their weaker (neutral current only) coupling to matter.

Inside the star, the neutrinos and antineutrinos undergo either partial or total flavor conversion depending on the mixing angle θ_{13} and on the mass hierarchy of the neutrino mass spectrum. The hierarchy is defined as *normal* (*inverted*) if the third mass eigenstate – the one whose electron component is $\sin^2 \theta_{13}$ – is the heaviest (lightest). The net conversion probability is due to a combination of effects of neutrino-neutrino coherent scattering [22,23,24,25,26,27,28,29,30,31,32,33,34,35,36] and of matter-driven resonant conversion (see e.g., [37,38,39]). The neutrino-neutrino effects swap the energy spectra of the electron and non-electron components of the flux for the inverted mass hierarchy and above a certain critical energy, E_c . Typical critical energies are below ~ 10 MeV (see e.g. [29]), with lower values for antineutrinos compared to neutrinos. The matter-driven conversion occurs more externally in the star and induces a further permutation of the energy spectra of the fluxes in the different flavors that enter the resonances.

The diffuse flux of supernova neutrinos in a detector is simply the sum of the contributions from the individual stars. This sum can be expressed as an integral involving the cosmological rate of supernovae, $R_{SN}(z)$, which is a function of the redshift z and is defined as the number of supernovae in the unit of comoving volume in the unit time. Starting with the present value, $R_{SN}(0) \sim \mathcal{O}(10^{-4})$ Mpc $^{-3}$ yr $^{-1}$, the rate increases with z and flattens at $z > 1$ (see e.g. [40]). In terms of R_{SN} , the DSN ν F in a detector at Earth, differential in energy, surface and time, is given by:

$$\Phi(E) = \frac{c}{H_0} \int_0^{z_{max}} R_{SN}(z) \frac{dN^{det}(E')}{dE'} \frac{dz}{\sqrt{\Omega_m(1+z)^3 + \Omega_\Lambda}} \quad (5)$$

(see e.g. [13]), where $dN^{det}(E')/dE'$ is the contribution of an individual supernova, inclusive of neutrino oscillations and of the redshift of energy, $E' = E(1+z)$. Ω_m and Ω_Λ are the fractions of the cosmic energy density in matter and dark energy respectively; c is the speed of light and H_0 is the Hubble constant.

Examples of calculated energy spectra for the $\bar{\nu}_e$ component of the DSN ν F are shown in fig. 1. We see that the flux peaks at $E_{max} = 3 - 7$ MeV, where it reaches typical values of $\mathcal{O}(1)$ cm $^{-2}$ s $^{-1}$ MeV $^{-1}$, and falls rapidly at $E \gg E_{max}$. It has been shown [43] that in this high energy regime, which is relevant for our analysis, the flux is approximated very well ($\sim 5\%$ accuracy or better) by an exponential:

$$\phi(E) \simeq \phi_0 e^{-E/E_0} \quad , \quad (6)$$

where the energy E_0 is close to the energy at the peak of the spectrum, $E_0 \sim E_{max}$. The total flux above a realistic detection threshold of 10-20 MeV is

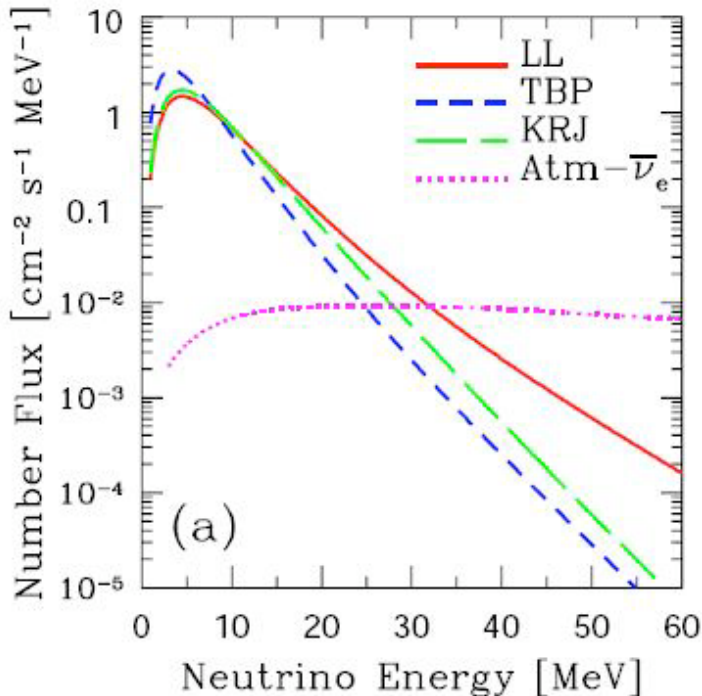


Fig. 1. Examples of energy spectra of the $\bar{\nu}_e$ component of the DSN ν F from the literature, specifically from the Garching (KRJ), Lawrence Livermore (LL) and Arizona (TBP) models, with oscillations (see also Table 1) [21,41,42,13]. The background due to atmospheric $\bar{\nu}_e$ is shown as well. This figure is taken from ref. [13], with permission.

larger for larger E_0 , and is proportional to the normalization of the supernova rate, R_{SN} . The large uncertainties on these two quantities translates into a large uncertainty on the DSN ν F.

In Table 1 we illustrate this by summarizing several published predictions of the $\bar{\nu}_e$ component of the DSN ν F. The Table gives the values of E_0 found by fitting the energy spectra with the simple exponential (6), and the predicted $\bar{\nu}_e$ flux above the SK threshold. In both columns we see large differences, due to the different input quantities and constraints that are used in calculating the DSN ν F. For example, to describe the DSN ν F energy spectrum some authors use neutrino spectra that result from calculations of neutrino transport (e.g., [21]), while others use spectra that fit the SN1987A data [15] or simply adopt thermal spectra with temperatures varying within indicative intervals [44]. This diversity of approaches results in the variation $E_0 = 3.8 - 8.5$ MeV, which we use in our analysis¹. An even larger variation is seen in the integrated flux,

¹ Even though the interval of E_0 given here refers to electron antineutrinos, we use it for other neutrino species as well, as a representative range, and for easier comparison between different channels.

model, reference and comments	E_0/MeV	$\Phi_{\bar{\nu}_e}(E > 19.3\text{MeV})$ ($\text{cm}^{-2}\text{s}^{-1}$)
LMA oscillations [10]	5.68	0.43
Galaxy evolution [6]	5.35	0.41
Constant SN rate [5]	5.62	3.1
Cosmic gas infall [7]	5.3	0.2
Cosmic chemical evolution [8] (“NC” model)	5.1	0.39
Heavy metal abundance [9]	5.1	< 2.2
SN1987A fit [15]	4 - 7	0.05-0.35 (99% C.L.)
SN1987A-inspired [45] (fig. 4 in [45])	3.8 - 5.8	$\sim 0.24 - 1.2$
“concordance” [11,44]	4.0 - 8.5	0.3-1.2
Chemical evolution, bimodal IMF [16]	not given	0.4 - 3.2
Garching code [21], with LMA oscillations [13] (fig. 1)	4.4	0.28
Lawrence Livermore code [41], with LMA oscillations [13] (fig. 1)	5.2	0.46
Arizona code [42], with LMA oscillations [13] (fig. 1)	3.9	0.14

Table 1

Summary of existing calculations of the $\bar{\nu}_e$ component of the DSN ν F. For each, we give the value of E_0 for which a simple exponential spectrum, Eq. (6), best fits the neutrino spectrum in the high energy regime ($E \gtrsim 10$ MeV). We also give the integrated flux above the SK energy threshold. The models in the first six rows are those considered in the SK analysis [1]. In several cases, the values quoted in the table have been inferred from graphics in the original references. The fluxes in ref. [13] are calculated up to a normalization factor, which is estimated to be of order unity.

which ranges from $\sim 0.05 \text{ cm}^{-2}\text{s}^{-1}$ to values exceeding the SK limit, eq. (1).

In closing this section, we would like to point out that the effects of neutrino-neutrino scattering on flavor conversion have been studied in detail only recently, and therefore they were not included in the literature we have referenced for the spectral shape, eq. (6), and for the results in figure 1 and in Table 1. While the inclusion of these effects is certainly in the agenda for the near future (see the initial study in [36]), we believe that the literature we

have quoted is still a good description for the purpose of this paper. Indeed, older results are still valid for the normal mass hierarchy, where neutrino-neutrino effects are negligible. Moreover, they can reproduce (with effective parameters) the case of inverted mass hierarchy with neutrino-neutrino scattering above the swap energy E_c . This is sufficient for our analysis, since E_c is typically below the energy windows of interest here, $E \gtrsim 10$ MeV (see Table 6; a possible exception is LENA at Wellington, as the table shows).

3 The data and the analysis

3.1 The data and their interpretation

We have used the electron-like events from the 1496 days of operation of SuperKamiokande, published in ref. [1] and described in more detail in [46]. Their energy distribution is shown in fig. 2. Due to the cuts motivated by background rejection, the events are limited to the interval 18 – 82 MeV in lepton energy.

The events could be due to neutrinos of different species. Considering only the dominant interaction channel for each species, we have the following possibilities (see also, e.g. [47]):

- (1) $\bar{\nu}_e$ interacting via inverse beta decay:



- (2) ν_e scattering on oxygen and on electrons:



(here X denotes all possible final states, $X = {}^{16}\text{F}, {}^{16}\text{F}^*, \dots$),

- (3) muon and tau neutrinos and antineutrinos scattering on electrons:



All these channels are indistinguishable in the detector because SK is not charge-sensitive, and so it does not discriminate between electrons and positrons. Moreover, since the DSN ν F is isotropic in space, one can not use angular information to separate elastic scattering events, in contrast with an individual neutrino burst.

In the natural assumption of similar luminosities in the different species (sec. 2.1), the process (7) largely dominates due to its larger cross section, hence the choice in ref. [1] to consider only this channel, obtaining a limit on the $\bar{\nu}_e$ component of the DSN ν F.

Here we study all the channels above, resulting in limits on the $\bar{\nu}_e$, ν_e , ν_x and $\bar{\nu}_x$ components of the DSN ν F. We do this by considering one neutrino species at a time, meaning that to derive the limit on the ν_e component of the DSN ν F we neglected the presence of all the other species, and likewise for the other components of the flux. While in contrast with theory, this is an acceptable working assumption, as it gives the most conservative upper limits.

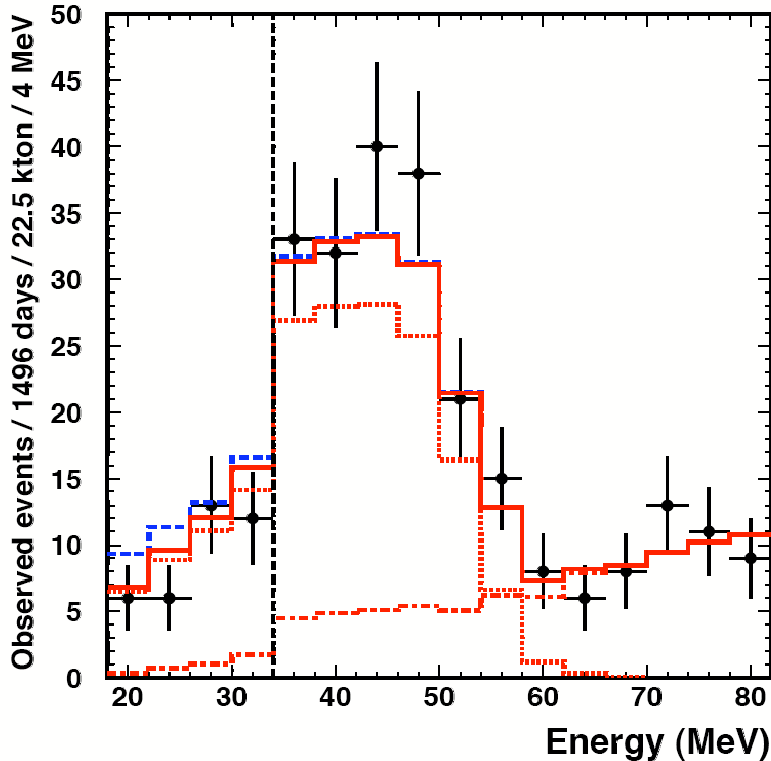


Fig. 2. The distribution in lepton energy of the SK events and of the fitted backgrounds. The dotted and dashed histograms below the solid one are the fitted backgrounds from invisible muons and atmospheric neutrinos (ν_e and $\bar{\nu}_e$) respectively. The solid histogram is the sum of these two backgrounds. The dashed line above the solid one shows the sum of the total background and of the 90% upper limit on the DSN ν F signal found in [1] for the $\bar{\nu}_e$ component of this flux. The figure is taken from ref. [46], with permission. Note that the figure published in [1] is corrected for efficiency, i.e., it does not include the cuts that motivate the realistic efficiency in Eq. (12).

3.2 The analysis

For each of the channels given in sec. 3.1, we performed a χ^2 analysis following the procedure used by the SK collaboration in [1,46], to which we refer for details. Briefly, the steps of the analysis are as follows:

- (1) We consider the events due to the DSN ν F (signal) and those due to two sources of background. These are invisible muons² and the flux of atmospheric ν_e 's and $\bar{\nu}_e$'s (figure 2). For each of these three components, we hold the spectral shape (taken from [46]) fixed and take the normalization as fit parameter. Therefore, we have three parameters, one of them being the DSN ν F normalization, ϕ_0 (Eq. (6)).
- (2) We calculate the χ^2 , which is a function of the three normalizations. It is given by the expression:

$$\chi^2 = \sum_{l=1}^{16} \frac{(-N_l^{data} + \phi_0 A_l + \beta B_l + \gamma C_l)^2}{(\sigma_l^{data})^2 + \sigma_{sys}^2} \quad (11)$$

where β and γ are normalization constants for invisible muons and for atmospheric electron neutrinos respectively. A_l , B_l and C_l are the number of events from the supernova flux, invisible muons and atmospheric neutrinos in the l bin. N_l^{data} is the number of events in the same bin; σ_l^{data} and σ_{sys} are the statistical and systematic errors, from [1,46].

- (3) We marginalize over the background normalizations and so obtain a function $\chi^2(\phi_0)$, which depends on the signal only.
- (4) From $\chi^2(\phi_0)$ we find the 90% C.L. limit on ϕ_0 . This limit is immediately translated into two more physically meaningful limits: one on the DSN ν F and another on the number of events due to it.
- (5) We repeat the procedure for different spectral shapes of the diffuse supernova flux, i.e. for different values of E_0 in the interval $E_0 = 3.8 - 8.5$ (Sec. 2).

To predict the histogram of events due to the DSN ν F, we have used the experimental efficiency as in [1,46]:

$$\epsilon(E_e) = \begin{cases} 0.47 & \text{if } E_e \leq 34 \text{ MeV;} \\ 0.79 & \text{if } E_e > 34 \text{ MeV.} \end{cases}, \quad (12)$$

² A muon that has too low energy to produce any Cerenkov light in water is called an *invisible muon*. Its only observable effect is the Cerenkov light from the electron produced by its decay. Invisible muons originate from the interaction of atmospheric neutrinos in the vicinity of the detector.

and the SuperKamiokande energy resolution as given in [48]:

$$\mathcal{E}(E_e) = 0.5 \text{ MeV} \sqrt{\frac{E_e}{\text{MeV}}}, \quad (13)$$

with E_e being the positron/electron energy.

Published nuclear cross sections were adopted. In particular, for inverse beta decay we followed Vissani and Strumia [49] (fig. 3). For the energy interval considered here, nucleon recoil is negligible, therefore the energy of the emitted positron simply differs by 1.29 MeV from the neutrino energy. The total cross section of ν_e scattering on oxygen was taken from [50], with the analytical form in [51] (fig. 3). Following the latter reference, we have assumed that the difference between electron energy and neutrino energy is 15 MeV in 100% of the cases³. For the scattering of all species on electrons, the Standard Model cross section was used at the lowest order in the fine structure constant (see e.g., [51]). Note that the difference between the energies of the incoming neutrino and of the scattered electron is not a constant in this case.

The analysis was restricted to the physical region, $\phi_0 \geq 0$, by normalizing the likelihood function to 1 in this semi-plane, as it is done in [1,46].

We found that the data are not constraining enough to have E_0 as an additional fit parameter, instead than a fixed quantity. That would mean having four fit variables, two for the DSN ν F and two for the background. This number of degrees of freedom is too large considering that the DSN ν F falls rapidly with energy, and therefore it is constrained mainly by the twelve events in the first two energy bins (fig. 2).

4 Results

We now present the results for each of the four channels, ν_e , $\bar{\nu}_e$, ν_x , $\bar{\nu}_x$. They are shown in the Tables 2-5, and in the figures 4-7. For each channel, we give both the 90% C.L. upper limit on the number of events, $N_{90\%}$, as well as the corresponding bound on the neutrino flux for certain intervals of neutrino energy.

While adequate overall, the exponential spectrum we use, Eq. (6), tends to overestimate the flux at low energy (see [43]). Therefore our upper limits for

³ This assumption has only a phenomenological, approximated validity. Improvements on this should come from detailed cross section calculations of neutrino scattering on oxygen, and have not been published so far.

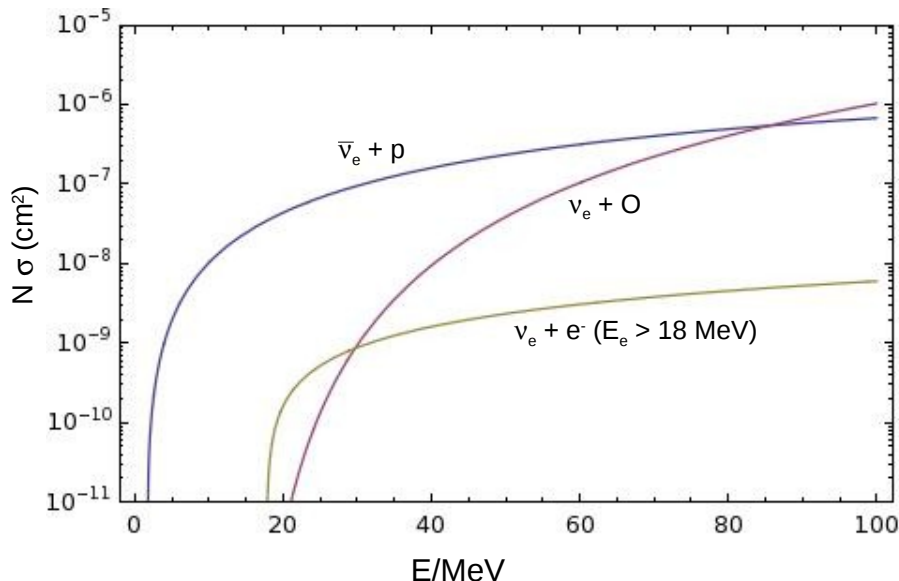


Fig. 3. The cross sections for the processes (7), (8) and (9), multiplied by the relevant numbers of scatterers in SuperKamiokande, as functions of the neutrino energy, E . The cross section for ν_e -electron scattering is integrated over the energy of the outgoing electron, E_e , under the condition that it exceeds the detector's threshold, $E_e > 18$ MeV. Note how, in spite of the smaller cross section, ν_e -electron scattering dominates over ν_e -oxygen interaction at $E \sim 20 - 30$ MeV, thanks to the larger number of scatterers. We used the number of protons $N_p = 1.5 \cdot 10^{33}$.

thresholds around 10 – 15 MeV are slightly more conservative than those that could be obtained with more realistic (but model-dependent) spectral shapes.

We do not present limits on the full fluxes (i.e., integrated over all energies) for two reasons. The first is that below $E \sim 10$ MeV the energy spectrum of the DSN ν F becomes more model dependent and therefore any bound could be given only for very specific scenarios of neutrino spectra and luminosities, supernova rate, etc., as done in [1]. The second reason is that the study of the full flux is out of the reach of current and planned experiments, due to background at low energy⁴.

⁴ Even liquid scintillator detectors [52,53], as well as the upgraded SK with the addition of Gadolinium [54], would be limited to a ~ 10 MeV threshold, due to the ineliminable background of reactor neutrinos. Lowering the threshold could be feasible if a detector becomes available in a region free from sources of nuclear power [53].

E_0/MeV	$N_{90\%}$	limit on $\Phi_{\bar{\nu}_e}$ ($\text{cm}^{-2}\text{s}^{-1}$)	
		$E/\text{MeV} > 11.3$	$E/\text{MeV} > 19.3$
3.5	4.89	13.4	1.37 (1.16)
5.35	6.62	6.88	1.49 (1.28)
5.5	6.86	6.41	1.52 (1.29)
6.5	8.40	5.56	1.62 (1.38)
7.5	10.19	5.01	1.75 (1.50)
8.5	12.31	4.87	1.90 (1.63)

Table 2

Upper limits for the $\bar{\nu}_e$ channel. We give the 90% C.L. bound for the number of events, $N_{90\%}$, and the corresponding limit on the flux of neutrinos above two different energy thresholds. The numbers in brackets in the second column were obtained using the less accurate cross section adopted in the SK analysis [1]; they are shown for comparison.

4.1 Results for $\bar{\nu}_e$

Our results for the $\bar{\nu}_e$ flux are summarized in Table 2 and fig. 4. They generalize the study of the SK collaboration [1], where only models with $E_0 \simeq 5.1 - 5.7$ MeV were considered. We give the flux limits above two thresholds of neutrino energy: $E_{thr} = 19.3$ MeV and $E_{thr} = 11.3$ MeV. The first corresponds to the energy window used in the SK analysis in [1], while the second is the expected threshold for SK upgraded with the addition of Gadolinium to the water [54] (see sec. 5).

The 90% C.L. bound on the number of events is in the range $N_{90\%} \sim 5 - 12$, and the corresponding upper limit on the flux above 19.3 MeV of neutrino energy is $\sim 1.4 - 1.9 \text{ cm}^{-2}\text{s}^{-1}$. Both the bounds on the flux and that on the number of events depend on E_0 monotonically, getting looser for larger E_0 . This agrees with intuition: with the decrease of E_0 the neutrino spectrum and the spectrum of the signal of observed electrons fall more rapidly with energy. This implies that the DSN ν F is constrained by the uncertainty on the number of events in the lowest one or two energy bins (see figure 2). In contrast, with a less steep spectrum (larger E_0) part of the signal could be in the higher energy bins, resulting in a looser constraint.

For the energy spectra used in the SK analysis [1], e.g., $E_0 = 5.35$ MeV, we obtained a limit that is about 25% looser than the SK result, Eq. (1): $\Phi_{\bar{\nu}_e}(E > 19.3 \text{ MeV}) \simeq 1.49 \text{ cm}^{-2}\text{s}^{-1}$, compared to $\Phi_{\bar{\nu}_e}(E > 19.3 \text{ MeV}) \simeq 1.2 \text{ cm}^{-2}\text{s}^{-1}$ of ref. [1]. We have checked that a 17% discrepancy is due to our using a more precise cross section for inverse beta decay, while the remaining

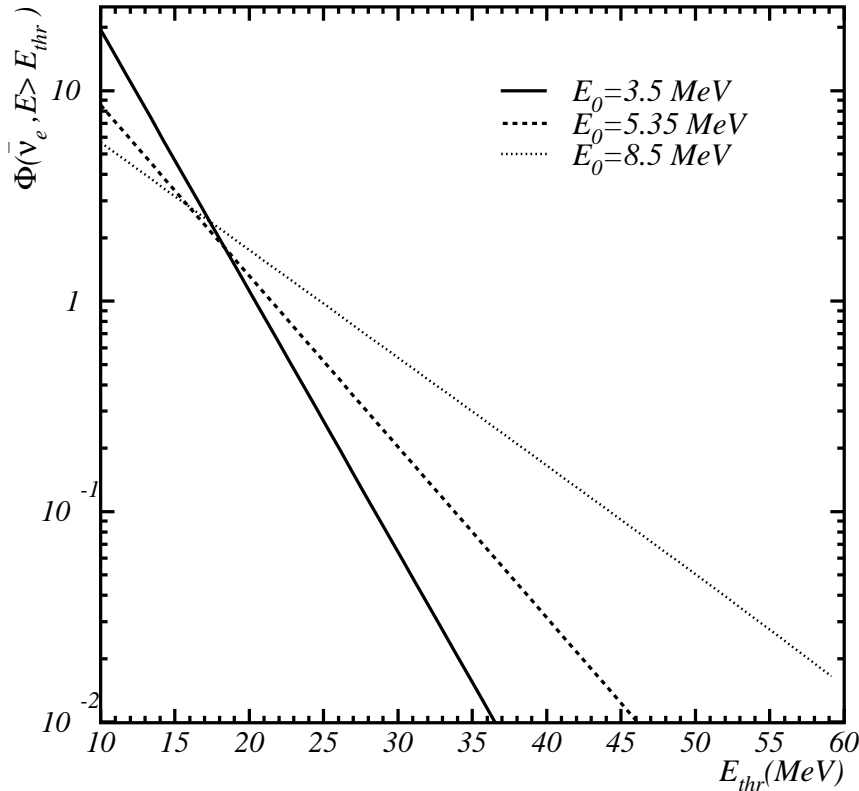


Fig. 4. The 90% C.L. upper limit on the $\bar{\nu}_e$ flux (in $\text{cm}^{-2}\text{s}^{-1}$) above a neutrino energy threshold E_{thr} , as a function of E_{thr} , for different values of E_0 .

8% difference should probably be attributed to details in the data analysis of the SK collaboration that we do not have access to. It should be considered as an error associated to the specific method of analysis used.

The upper limit on the diffuse flux of $\bar{\nu}_e$ above 11.3 MeV varies between $\sim 4.9 - 13.4 \text{ cm}^{-2}\text{s}^{-1}$. The allowed flux is larger for smaller E_0 , i.e., for steeper spectrum: indeed, a spectrum that falls rapidly in energy allows a large flux below the SK threshold, while still giving a sufficiently small number of events in the SK energy window.

Figure 4 completes the description of the $\bar{\nu}_e$ flux bounds, by showing how these vary with the energy interval, which was taken of the form $[E_{thr}, \infty]$. This figure is of guidance for experimental projects that may have different energy threshold than SK. Notice how around $E_{thr} \sim 20$ MeV the flux limit has little dependence on E_0 ⁵. This because $E_{thr} \sim 20$ MeV corresponds to

⁵ We did not find a value of E_{thr} for which the dependence on E_0 is null. The curves in fig. 4, as well as those for other channels, figs. 5-7, do *not* meet in one point, even though the figures might give such illusion due to the use of the logarithmic scale.

E_0/MeV	$N_{90\%}$	limit on Φ_{ν_e} ($\text{cm}^{-2}\text{s}^{-1}$)		
		$E/\text{MeV} > 11.3$	$22.9 < E/\text{MeV} < 36.9$	$E/\text{MeV} > 19.3$
3.5	4.80	$1.51 \cdot 10^3$	53.9	$1.54 \cdot 10^2$
3.8	5.17	$1.16 \cdot 10^3$	53.4	$1.41 \cdot 10^2$
5.35	8.86	$4.27 \cdot 10^2$	45.3	95.8
5.5	9.41	$3.99 \cdot 10^2$	44.6	93.1
6.5	14.4	$2.77 \cdot 10^2$	41.0	80.8
7.5	23.5	$2.20 \cdot 10^2$	39.6	75.7
8.5	33.3	$1.88 \cdot 10^2$	38.8	73.3

Table 3

The same as Tab. 2 for the ν_e channel.

the interval of the SK analysis, and for this reason it is the most strongly constrained. Due to the exponential dependence of the DSN ν F on energy, a small variation of the flux – within the statistical errors of SK – at 20-30 MeV corresponds to a large variation of the same flux at lower or higher energy, and this explains the strong dependence of the bounds on E_0 for E_{thr} substantially different from 20 MeV.

4.2 Results for ν_e

The upper limits on the ν_e component of the DSN ν F, and on the associated number of events, are given in Table 3 and fig. 5. In Table 3 we present the limits for the ν_e flux above 11.3 MeV and 19.3 MeV to allow direct comparison with the $\bar{\nu}_e$ channel, where these thresholds are most relevant. We also give results for the same energy window of the SNO search, $E = 22.9 - 36.9$ MeV, also for the purpose of comparison.

Similarly to the $\bar{\nu}_e$ channel, we see that larger E_0 corresponds to looser limit on the number of events, which can be as high as ~ 33 . The upper bound on the flux of ν_e is $1.5 \cdot 10^3 \text{ cm}^{-2}\text{s}^{-1}$ ($1.5 \cdot 10^2 \text{ cm}^{-2}\text{s}^{-1}$) above 11.3 MeV (19.3 MeV). It is about two orders of magnitude larger than the limit on the $\bar{\nu}_e$ flux in the same energy interval, due to the smaller detection cross section. Besides the overall scale, the ν_e cross section (total of both detection processes) differs from that of inverse beta decay in its rising faster with energy. This implies a less steep fall of the spectrum of the observed leptons, and therefore an increased possibility to have DSN ν F events distributed in the high energy bins within the statistical errors. That is why the limits on the numbers of events are generally looser for ν_e . The same difference in the energy dependence of the

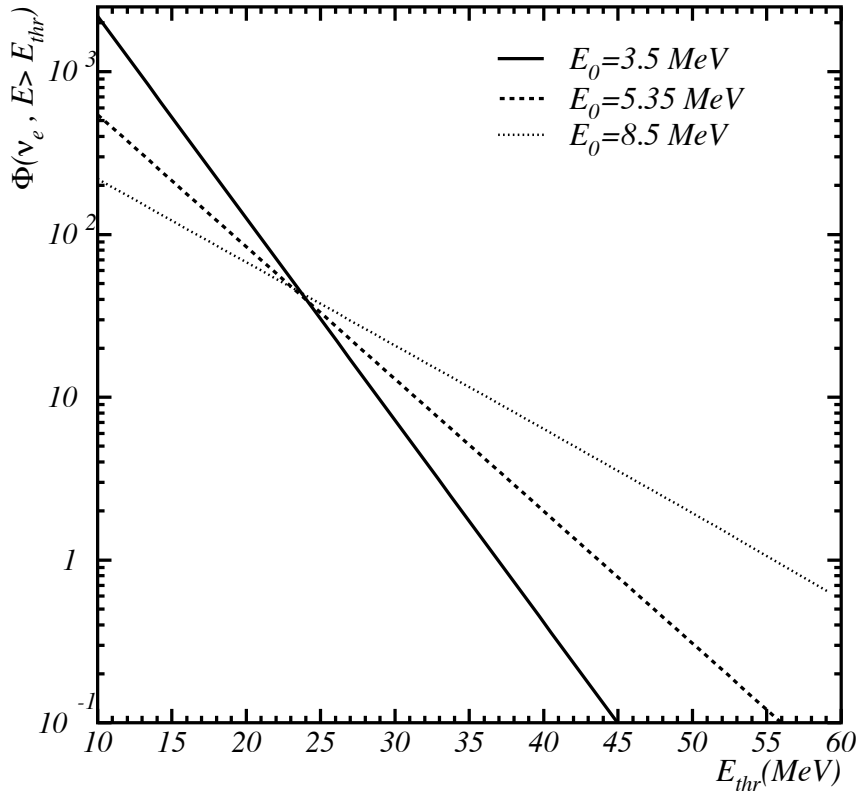


Fig. 5. The same as fig. 4 for ν_e .

cross section explains why in the ν_e channel the correlation between lower E_0 and larger flux allowed is more pronounced.

In the interval $E = 22.9 - 36.9$ MeV we find the ν_e flux to be smaller than $54 \text{ cm}^{-2}\text{s}^{-1}$. Such constraint improves on the SNO result in the same interval, Eq. (3), and therefore represents the best *direct* bound to date.

We refer to Fig. 5 for the bounds in other energy intervals; the qualitative features of the figure are similar to those of fig. 4.

4.3 Results for ν_x and $\bar{\nu}_x$

The upper bounds on $N_{90\%}$ and on the flux for ν_x and $\bar{\nu}_x$, shown in Tables 4 and 5, and figures 6 and 7, are of the same order of magnitude, with small differences reflecting differences in the cross sections of neutrinos and antineutrinos. For $E > 19.3$ MeV (Tables 4 and 5) the limit on the flux is $\sim (1.0 - 1.35) \cdot 10^3 \text{ cm}^{-2}\text{s}^{-1}$ for ν_x and $\sim (1.3 - 1.8) \cdot 10^3 \text{ cm}^{-2}\text{s}^{-1}$ for $\bar{\nu}_x$. These improve by about four orders of magnitude on the previous best limits from

E_0/MeV	$N_{90\%}$	limit on Φ_{ν_x} ($\text{cm}^{-2}\text{s}^{-1}$)	
		$E/\text{MeV} > 11.3$	$E/\text{MeV} > 19.3$
3.5	4.38	$1.32 \cdot 10^4$	$1.35 \cdot 10^3$
3.8	4.51	$1.08 \cdot 10^4$	$1.31 \cdot 10^3$
5.35	5.24	$5.29 \cdot 10^3$	$1.18 \cdot 10^3$
5.5	5.32	$4.99 \cdot 10^3$	$1.17 \cdot 10^3$
6.5	5.87	$3.78 \cdot 10^3$	$1.11 \cdot 10^3$
7.5	6.45	$3.08 \cdot 10^3$	$1.06 \cdot 10^3$
8.5	7.06	$2.66 \cdot 10^3$	$1.02 \cdot 10^3$

Table 4
The same as Tab. 2 for ν_x .

E_0/MeV	$N_{90\%}$	limit on $\Phi_{\bar{\nu}_x}$ ($\text{cm}^{-2}\text{s}^{-1}$)	
		$E/\text{MeV} > 11.3$	$E/\text{MeV} > 19.3$
3.5	4.38	$1.74 \cdot 10^4$	$1.77 \cdot 10^3$
3.8	4.51	$1.41 \cdot 10^4$	$1.72 \cdot 10^3$
5.35	5.22	$6.81 \cdot 10^3$	$1.53 \cdot 10^3$
5.5	5.30	$6.48 \cdot 10^3$	$1.51 \cdot 10^3$
6.5	5.82	$4.88 \cdot 10^3$	$1.43 \cdot 10^3$
7.5	6.40	$3.96 \cdot 10^3$	$1.36 \cdot 10^3$
8.5	7.00	$3.35 \cdot 10^3$	$1.31 \cdot 10^3$

Table 5
The same as Tab. 2 for $\bar{\nu}_x$.

LSD, Eq. (4), which refer to the interval 20 – 100 MeV.

Due to the rough equipartition of energy among the six neutrino species predicted by theory, it is reasonable to expect the ν_x and $\bar{\nu}_x$ components of the DSN ν F to be comparable to the electron flavor ones, that are more strongly constrained. Therefore, the direct limits we found here for ν_x and $\bar{\nu}_x$, while being the best available, are probably far from realistic values of these fluxes. They are nevertheless important for their observational, model-independent character, and as a reference for future, more sensitive, searches.

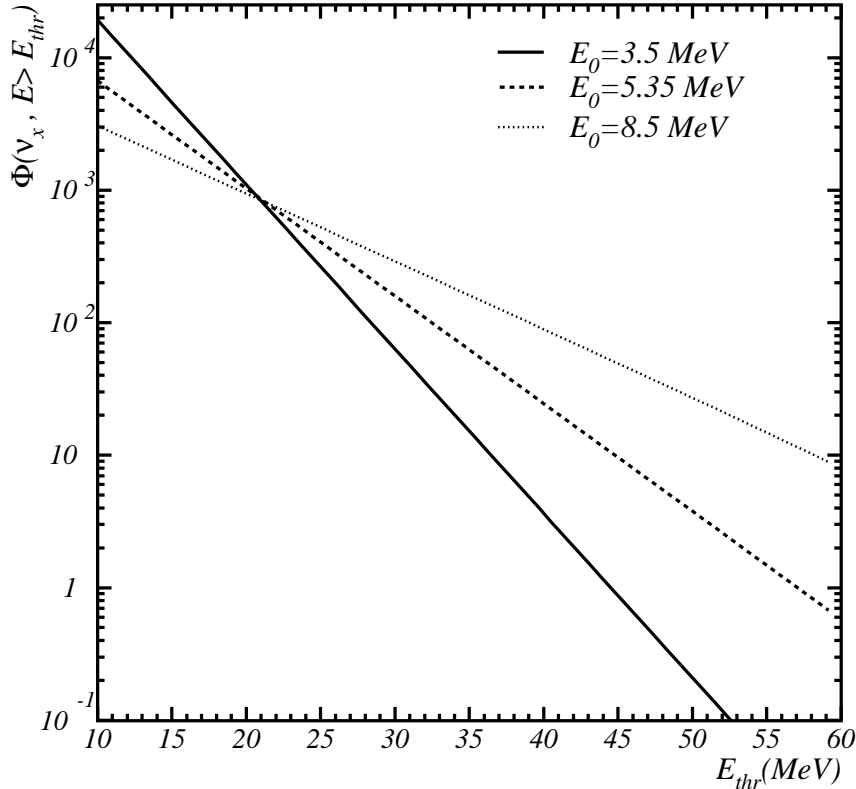


Fig. 6. The same as fig. 4 for ν_x .

4.4 Interpretation of the results: luminosity bounds

What constraints can be drawn from our results on the neutrino emission from a supernova? A full address of this question requires a detailed analysis of all the uncertainties, which we do not perform here. However, as an example we study what can be concluded on the neutrino luminosity if the supernova rate is known, which is likely to be the case in the near future, after data from SNAP [55] and JWST [56] become available.

To extract the luminosity in a given flavor of an individual neutrino burst, one needs to go beyond the simple parametrization of the diffuse flux in Eq. (6). We use the analytical description by Lunardini [43], which is valid within a few per cent above the SK threshold and is obtained from Eq. (5) with a power law form of R_{SN} and a neutrino spectrum at the exit of the star (after oscillations) of the form of an exponential times a power law [21]. It reads:

$$\Phi \simeq \frac{R_{SN}(0)Lc}{H_0\Gamma(2+\alpha)E_0^2} \left(\frac{E}{E_0}\right)^{\alpha-\eta-1} \left(\Gamma\left[\eta+1, \frac{E}{E_0}\right] - \Gamma\left[\eta+1, (1+z_{max})\frac{E}{E_0}\right]\right), \quad (14)$$

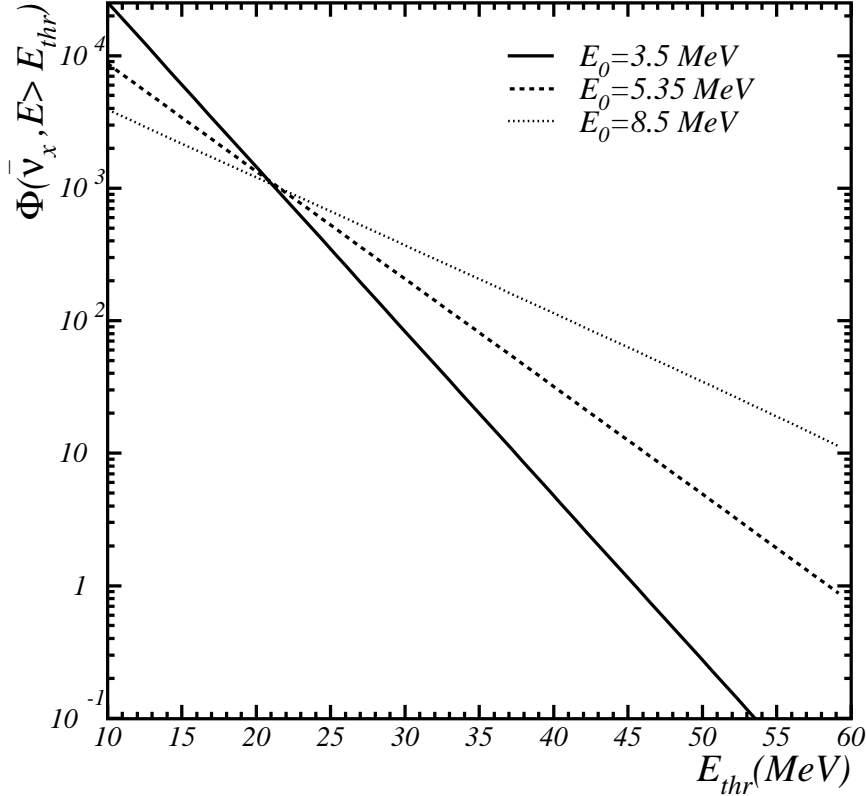


Fig. 7. The same as fig. 4 for $\bar{\nu}_x$.

where L is the total energy (in the individual flavor) of the neutrino burst leaving the star, and $\alpha \simeq 2 - 5$ is a parameter describing its spectral shape [43]. The average energy of the neutrinos leaving the star is $\langle E \rangle \simeq E_0(1 + \alpha)$. We have $\eta = \alpha + \beta - 3\Omega_m/2$, where β describes the cosmological supernova rate: $R_{SN} \simeq (1+z)^\beta$. $z_{max} \sim 1$ is a break in the redshift distribution of supernovae. We fix R_{SN} to be the best piecewise fit to the data found by Beacom and Hopkins [40]: $R_{SN} \simeq 2.0 \cdot 10^{-4} \text{ yr}^{-1} \text{ Mpc}^{-3}$, $\beta = 3.28$ and $z_{max} = 1.0$. While Eqs. (6) and (14) differ only minimally in the energy dependence [43], the second is more adequate for our purpose because in it the dependence on the different parameters is explicit.

For every value of E_0 and α , the combination of Eq. (14) and of our flux limits (Tables 2-5) gives an upper limit on the integrated luminosity L , which can then be compared to the theoretical expectation of $L \sim 5 \cdot 10^{52}$ ergs per neutrino flavor.

Results are shown in fig. 8, where we have imposed $9 < \langle E \rangle / \text{MeV} < 24$ as naturalness constraint (solid curves). We see that, for $E_0 \gtrsim 5.5$ MeV, the upper limit on the $\bar{\nu}_e$ luminosity approaches, or even crosses, the theoretically

interesting range, an intriguing fact that has been already observed in [57]. Softer neutrino spectra, however, allow neutrino the neutrino luminosity to be several times larger than the theoretical central value. This is expected, since softer neutrino spectrum means smaller fraction of the total energy above the SK threshold. A further loosening of the luminosity constraint is expected if the uncertainty on the supernova rate is included [15].

The luminosity bounds for the other neutrino species are far from the theoretical range, reflecting the weaker flux limits. They could be useful to constrain the presence hidden sources that could add to the expected supernova neutrino flux.

5 Summary and discussion

We have analyzed the data of the search for the diffuse supernova neutrino flux published by the SK collaboration in 2003 [1]. Our work extends the analysis of collaboration itself in a number of ways. First, it considers all the relevant channels, one at a time (i.e., with all the signal attributed to a certain channel), resulting in bounds on the fluxes of all the neutrino species. Second, it takes into account a wider range of neutrino spectra, including the softer ones that have been suggested in the literature recently (Table 1). It also uses a more precise cross section for inverse beta decay, that rises more slowly with energy and therefore implies a looser bound on the $\bar{\nu}_e$ component of the flux. Results have been given for several different energy intervals motivated by near future experiments.

A first result is that the flux of $\bar{\nu}_e$ is bound, at 90% CL, to be smaller than $1.4 - 1.9 \text{ cm}^{-2}\text{s}^{-1}$ for $E > 19.3 \text{ MeV}$ and than $4.9 - 13.4 \text{ cm}^{-2}\text{s}^{-1}$ above a 11.3 MeV threshold. The flux intervals account for the variation with the neutrino energy spectrum, and the discrepancy with the SK limit, Eq. (1), is explained by the different cross section used, up to a minor 8% difference.

The limits in the ν_e channel improve on the previous limit from SNO, Eq. (3): at 90% C.L. the ν_e flux must be smaller than $54 \text{ cm}^{-2}\text{s}^{-1}$ in the interval $22.9 - 36.9 \text{ MeV}$ even for the softest neutrino spectrum, which represents the most optimistic case. The flux is allowed to be as large as $\mathcal{O}(10^2) \text{ cm}^{-2}\text{s}^{-1}$ ($\mathcal{O}(10^3) \text{ cm}^{-2}\text{s}^{-1}$) above 19.3 (11.3) MeV energy.

The upper limits on the non-electron species are in the range of $\mathcal{O}(10^3) \text{ cm}^{-2}\text{s}^{-1}$ to $\mathcal{O}(10^4) \text{ cm}^{-2}\text{s}^{-1}$ for the same two thresholds, and improve by several orders of magnitude over the previous bounds from LSD, Eq. (4).

Our results represents the most one can get from this generation of detectors

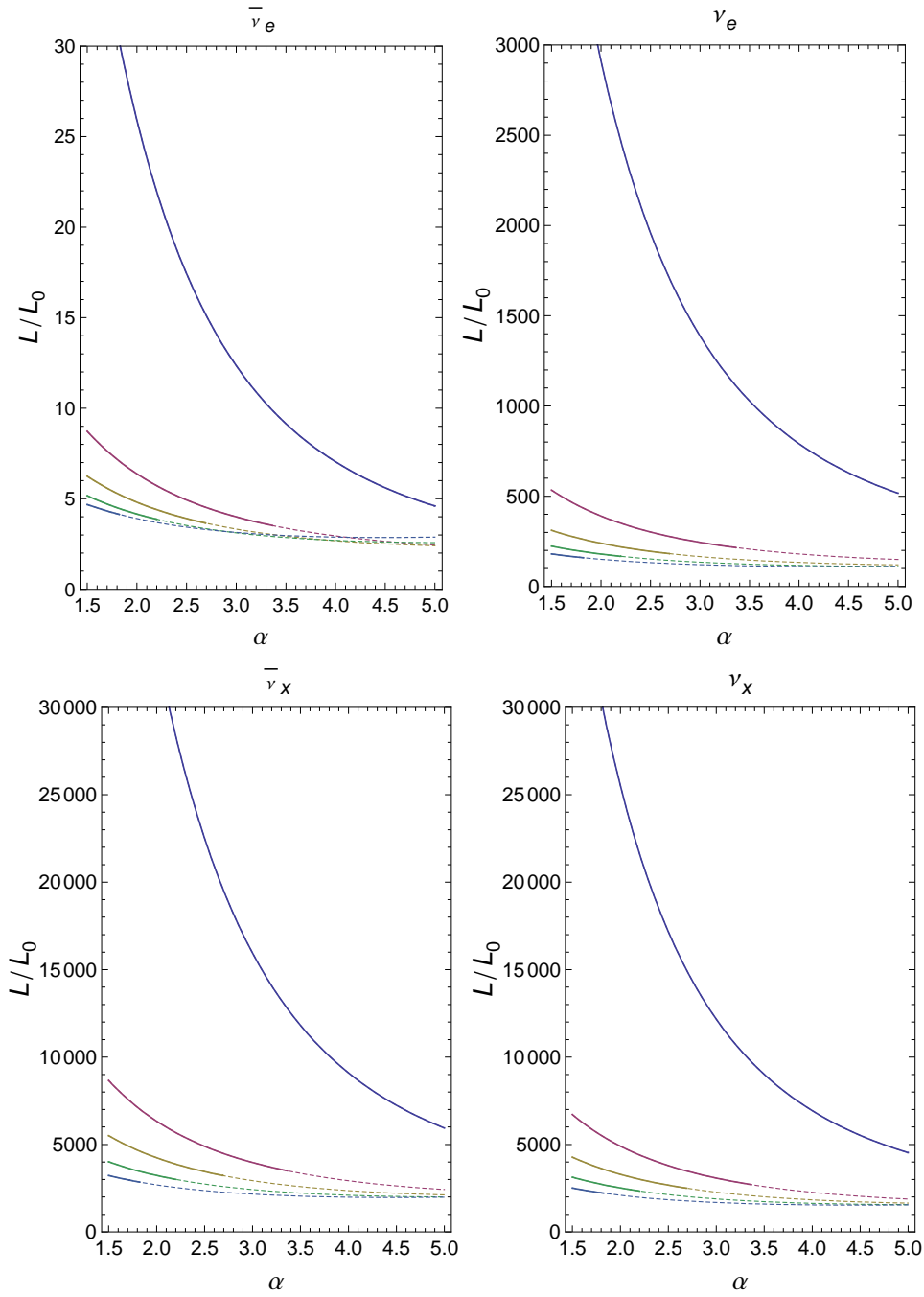


Fig. 8. 90% C.L. upper limits on the neutrino luminosity (in units of $L_0 = 10^{52}$ ergs) in the different species at the exit of the star, as a function of the “shape” parameter α . The curves, from upper to lower, correspond to $E_0/\text{MeV} = 3.5, 5.5, 6.5, 7.5, 8.5$ in every panel. The solid curves were obtained by imposing a naturalness condition on the average energy of the neutrino spectrum at the exit of the star: $9 < \langle E \rangle / \text{MeV} < 24$. Notice the large difference in the vertical scales between the different panels.

concept	channel	name of project	energy (MeV)	SK flux limit ($\text{cm}^{-2}\text{s}^{-1}$)
liquid scintillator	$\bar{\nu}_e$	LENA [53] (at Phyäsalmi)	9.5-30	5.5 – 22.3
liquid scintillator	$\bar{\nu}_e$	LENA [53] (at Wellington)	8.2-27.2	6.3 – 32
water	$\bar{\nu}_e$	HyperKamiokande, UNO, MEMPHYS (generic) [59,60,61]	19.3-80	1.4 – 1.9
water+Gd	$\bar{\nu}_e$	GADZOOKS (at Kamioka) [62]	15-30	2.6 – 4.6
water + Gd	$\bar{\nu}_e$	GADZOOKS (generic) [54]	11.3-80	5 – 13
liquid argon	ν_e	GLACIER, LANDD [63,64,65]	16-40	$(3.9 – 8.2) \cdot 10^2$

Table 6

Flux limits from SK at 90% C.L. for the energy intervals and channels that are relevant to the four most discussed future DSN ν F detectors (see text for details). We distinguish between generic designs and detailed studies that include estimates of the background at specific sites (see Table 8 in [62]). The intervals in the flux correspond to varying the neutrino spectrum in the range shown in Table 1.

on the diffuse flux, up to minor improvements that might come from increased statistics at SuperKamiokande (see the preliminary results in [58]). Considering that theoretical predictions of the DSN ν F in each neutrino species range from touching the current SK limit for $\bar{\nu}_e$ down to values 20 times smaller (Tab. 1), it is clear that SK might not be able to see the DSN ν F in the $\bar{\nu}_e$ channel and almost certainly will never detect it in other channels. This strongly reinforces the already strong case for new detectors with enhanced sensitivity to the DSN ν F.

With this in mind, we have given constraints on the flux in different energy intervals that could be relevant for future searches. They represent the minimum sensitivity that these searches should have to improve on the current status. To summarize, and also to add detail, in Table 6 we give the SK bound on the DSN ν F for the specific setup (neutrino species and energy interval) of the four different concepts that are most discussed for the future. These are a Megaton water Cerenkov detector [59,60,61], a 50 kt liquid scintillator experiment [52,53], a liquid Argon chamber [64,65] and the SK tank with Gadolinium trichloride dissolved in it [54]. For some projects, we consider both generic and site-specific designs, for which the background, and therefore the energy window of sensitivity, have been calculated in detail⁶. From the Table one

⁶ The energy intervals for the site-specific designs are nevertheless tentative, be-

can immediately see how crucial it is to have a detection threshold as low as possible, since the $\text{DSN}\nu\text{F}$ falls exponentially with energy.

The SK bounds in Table 6 will certainly be a practical benchmark for the planning of future detectors, as they allow to give a quantitative estimate of how much a given design will improve over SK. Moreover, our bounds will be an important component of a global analysis of multiple data sets once new data are available from different experiments.

We conclude with the comment that the detection of the diffuse flux of supernova neutrinos is an opportunity that the underground science community can not afford to miss, because of its implications for fundamental physics and astrophysics/cosmology. Since the flux is continuous in time, the barrier to its observation is only technological. Once the barrier is overcome, the experimental study of supernova neutrinos will transition from the realm of rare event to that of regular, ongoing data taking and analysis. Our results represent the status of the art of current searches and the ultimate sensitivity – up to minor improvements – of the existing detectors. It marks where the present generation of experiments leaves off and the new one will take on, in the next decade or so, to bring this field to maturity.

Acknowledgments

C.L. acknowledges support from the ORNL grant of the Institute of Nuclear Theory (INT) of Seattle, where this work was initiated, from Arizona State University, and from the RIKEN BNL Research Center (RBRC). O.L.G. Peres acknowledges support from FAPESP, CNPq and FAEPEX; he is grateful to the INT for hospitality. We are especially indebted to M.S. Malek and R.J. Wilkes for useful exchanges.

References

- [1] **Super-Kamiokande** Collaboration, M. Malek *et al.*, *Search for supernova relic neutrinos at super-kamiokande*, *Phys. Rev. Lett.* **90** (2003) 061101 [[hep-ex/0209028](#)].
- [2] G. S. Bisnovatyi-Kogan and Z. F. Seidov, *Medium-energy neutrinos in the universe*, *Soviet Astronomy (Tr: A. Zhurn.)* **26** (132) 1982.

cause they depend on the luminosity and spectrum of the $\text{DSN}\nu\text{F}$. Rather than optimal intervals, they should be considered as likely choices that an experimental collaboration would adopt for a data analysis.

- [3] L. M. Krauss, S. L. Glashow and D. N. Schramm, *Antineutrino astronomy and geophysics*, *Nature* **310** (1984) 191–198.
- [4] S. E. Woosley, J. R. Wilson and R. Mayle, *Gravitational collapse and the cosmic antineutrino background*, *Astrophys. Jour., Part 1* **302** (1986) 19–34.
- [5] T. Totani and K. Sato, *Spectrum of the relic neutrino background from past supernovae and cosmological models*, *Astropart. Phys.* **3** (1995) 367–376 [astro-ph/9504015].
- [6] T. Totani, K. Sato and Y. Yoshii, *Spectrum of the supernova relic neutrino background and evolution of galaxies*, *Astrophys. J.* **460** (1996) 303–312 [astro-ph/9509130].
- [7] R. A. Malaney, *Evolution of the cosmic gas and the relic supernova neutrino background*, *Astropart. Phys.* **7** (1997) 125–136 [astro-ph/9612012].
- [8] D. H. Hartmann and S. E. Woosley, *The cosmic supernova neutrino background*, *Astropart. Phys.* **7** (1997) 137–146.
- [9] M. Kaplinghat, G. Steigman and T. P. Walker, *The supernova relic neutrino background*, *Phys. Rev.* **D62** (2000) 043001 [astro-ph/9912391].
- [10] S. Ando, K. Sato and T. Totani, *Detectability of the supernova relic neutrinos and neutrino oscillation*, *Astropart. Phys.* **18** (2003) 307–318 [astro-ph/0202450].
- [11] L. E. Strigari, M. Kaplinghat, G. Steigman and T. P. Walker, *The supernova relic neutrino backgrounds at kamland and super-kamiokande*, *JCAP* **0403** (2004) 007 [astro-ph/0312346].
- [12] S. Ando, *Cosmic star formation history and the future observation of supernova relic neutrinos*, *Astrophys. J.* **607** (2004) 20–31 [astro-ph/0401531].
- [13] S. Ando and K. Sato, *Relic neutrino background from cosmological supernovae*, *New J. Phys.* **6** (2004) 170 [astro-ph/0410061].
- [14] F. Iocco, G. Mangano, G. Miele, G. G. Raffelt and P. D. Serpico, *Diffuse cosmic neutrino background from population III stars*, *Astropart. Phys.* **23** (2005) 303–312 [astro-ph/0411545].
- [15] C. Lunardini, *The diffuse supernova neutrino flux, star formation rate and sn1987a*, *Astropart. Phys.* **26** (2006) 190–201 [astro-ph/0509233].
- [16] F. Daigne, K. A. Olive, P. Sandick and E. Vangioni, *Neutrino signatures from the first stars*, *Phys. Rev.* **D72** (2005) 103007 [astro-ph/0509404].
- [17] C. Lunardini, *The diffuse supernova neutrino flux*, astro-ph/0610534.
- [18] C. Lunardini, *The diffuse neutrino flux from supernovae: Upper limit on the electron neutrino component from the non-observation of antineutrinos at superkamiokande*, *Phys. Rev.* **D73** (2006) 083009 [hep-ph/0601054].

- [19] SNO Collaboration, B. Aharmim *et al.*, *A search for neutrinos from the solar hep reaction and the diffuse supernova neutrino background with the sudbury neutrino observatory*, *Astrophys. J.* **653** (2006) 1545–1551 [[hep-ex/0607010](#)].
- [20] M. Aglietta *et al.*, *Limits on low-energy neutrino fluxes with the mont blanc liquid scintillator detector*, *Astropart. Phys.* **1** (1992) 1–9.
- [21] M. T. Keil, G. G. Raffelt and H.-T. Janka, *Monte carlo study of supernova neutrino spectra formation*, *Astrophys. J.* **590** (2003) 971–991 [[astro-ph/0208035](#)].
- [22] H. Duan, G. M. Fuller and Y.-Z. Qian, *Collective neutrino flavor transformation in supernovae*, *Phys. Rev.* **D74** (2006) 123004 [[astro-ph/0511275](#)].
- [23] H. Duan, G. M. Fuller, J. Carlson and Y.-Z. Qian, *Simulation of coherent non-linear neutrino flavor transformation in the supernova environment. i: Correlated neutrino trajectories*, *Phys. Rev.* **D74** (2006) 105014 [[astro-ph/0606616](#)].
- [24] S. Hannestad, G. G. Raffelt, G. Sigl and Y. Y. Y. Wong, *Self-induced conversion in dense neutrino gases: Pendulum in flavour space*, *Phys. Rev.* **D74** (2006) 105010 [[astro-ph/0608695](#)].
- [25] H. Duan, G. M. Fuller, J. Carlson and Y.-Z. Qian, *Analysis of collective neutrino flavor transformation in supernovae*, *Phys. Rev.* **D75** (2007) 125005 [[astro-ph/0703776](#)].
- [26] G. G. Raffelt and A. Y. Smirnov, *Self-induced spectral splits in supernova neutrino fluxes*, *Phys. Rev.* **D76**,(2007) 081301 [Erratum-*ibid.* **D77**, (2008) 029903], [[arXiv:0705.1830](#) [[hep-ph](#)]].
- [27] H. Duan, G. M. Fuller and Y.-Z. Qian, *A Simple Picture for Neutrino Flavor Transformation in Supernovae*, *Phys. Rev.* **D76** (2007) 085013 [[arXiv:0706.4293](#) [[astro-ph](#)]].
- [28] H. Duan, G. M. Fuller, J. Carlson and Y.-Z. Qian, *Neutrino Mass Hierarchy and Stepwise Spectral Swapping of Supernova Neutrino Flavors*, *Phys. Rev. Lett.* **99** (2007) 241802 [[arXiv:0707.0290](#) [[astro-ph](#)]].
- [29] G. L. Fogli, E. Lisi, A. Marrone and A. Mirizzi, *Collective neutrino flavor transitions in supernovae and the role of trajectory averaging*, *JCAP* **0712**, (2007) 010 [[arXiv:0707.1998](#) [[hep-ph](#)]].
- [30] G. G. Raffelt and A. Y. Smirnov, *Adiabaticity and spectral split in collective neutrino transformations*, *Phys. Rev.* **D76** (2007) 125008 [[arXiv:0709.4641](#) [[hep-ph](#)]].
- [31] H. Duan, G. M. Fuller, J. Carlson and Y. Z. Qian, *Flavor Evolution of the Neutronization Neutrino Burst from an O-Ne-Mg Core-Collapse Supernova*, *Phys. Rev. Lett.* **100**, 021101 (2008) [[arXiv:0710.1271](#) [[astro-ph](#)]].

- [32] A. Esteban-Pretel, S. Pastor, R. Tomas, G. G. Raffelt and G. Sigl, *Decoherence in supernova neutrino transformations suppressed by deleptonization*, *Phys. Rev.* **D76**, 125018 (2007) [arXiv:0706.2498 [astro-ph]].
- [33] A. Esteban-Pretel, S. Pastor, R. Tomas, G. G. Raffelt and G. Sigl, *Mu-tau neutrino refraction and collective three-flavor transformations in supernovae*, *Phys. Rev.* **D77**, 065024 (2008) [arXiv:0712.1137 [astro-ph]].
- [34] B. Dasgupta and A. Dighe, *Collective three-flavor oscillations of supernova neutrinos*, *Phys. Rev. D* **77**, 113002 (2008), arXiv:0712.3798 [hep-ph].
- [35] B. Dasgupta, A. Dighe, A. Mirizzi and G. G. Raffelt, *Spectral split in prompt supernova neutrino burst: Analytic three-flavor treatment*, *Phys. Rev.* **D77**, 113007 (2008), arXiv:0801.1660 [hep-ph].
- [36] S. Chakraborty, S. Choubey, B. Dasgupta and K. Kar, *Effect of Collective Flavor Oscillations on the Diffuse Supernova Neutrino Background*, arXiv:0805.3131 [hep-ph].
- [37] S. P. Mikheev and A. Y. Smirnov, *Neutrino oscillations in a variable-density medium and ν -bursts due to the gravitational collapse of stars*, *Sov. Phys. JETP* **64** (1986) 4–7 [arXiv:0706.0454 [hep-ph]].
- [38] A. S. Dighe and A. Y. Smirnov, *Identifying the neutrino mass spectrum from the neutrino burst from a supernova*, *Phys. Rev.* **D62** (2000) 033007 [hep-ph/9907423].
- [39] C. Lunardini and A. Y. Smirnov, *Probing the neutrino mass hierarchy and the 13-mixing with supernovae*, *JCAP* **0306** (2003) 009 [hep-ph/0302033].
- [40] A. M. Hopkins and J. F. Beacom, *On the normalisation of the cosmic star formation history*, *Astrophys. J.* **651** (2006) 142 [Erratum-ibid. **682** (2008) 1486] [astro-ph/0601463].
- [41] T. Totani, K. Sato, H. E. Dalhed and J. R. Wilson, *Future detection of supernova neutrino burst and explosion mechanism*, *Astrophys. J.* **496** (1998) 216–225 [astro-ph/9710203].
- [42] T. A. Thompson, A. Burrows and P. A. Pinto, *Shock breakout in core-collapse supernovae and its neutrino signature*, *Astrophys. J.* **592** (2003) 434 [astro-ph/0211194].
- [43] C. Lunardini, *Testing neutrino spectra formation in collapsing stars with the diffuse supernova neutrino flux*, *Phys. Rev.* **D75** (2007) 073022 [astro-ph/0612701].
- [44] J. F. Beacom and L. E. Strigari, *New test of supernova electron neutrino emission using sudbury neutrino observatory sensitivity to the diffuse supernova neutrino background*, *Phys. Rev.* **C73** (2006) 035807 [hep-ph/0508202].

- [45] M. Fukugita and M. Kawasaki, *Constraints on the star formation rate from supernova relic neutrino observations*, *Mon. Not. Roy. Astron. Soc.* **340** (2003) L7 [[astro-ph/0204376](#)].
- [46] M. S. Malek, *A search for supernova relic neutrinos* (2003), UMI-31-06530 available at <http://www-sk.icrr.u-tokyo.ac.jp/sk/pub/index.html>.
- [47] C. Volpe and J. Welzel, *Supernova Relic Electron Neutrinos and anti-Neutrinos in future Large-scale Observatories*, [[arXiv:0711.3237](#)] [[astro-ph](#)].
- [48] J. N. Bahcall, P. I. Krastev and E. Lisi, *Neutrino oscillations and moments of electron spectra*, *Phys. Rev.* **C55** (1997) 494–503 [[nucl-ex/9610010](#)].
- [49] A. Strumia and F. Vissani, *Precise quasielastic neutrino nucleon cross section*, *Phys. Lett.* **B564** (2003) 42–54 [[astro-ph/0302055](#)].
- [50] E. Kolbe, K. Langanke and P. Vogel, *Estimates of weak and electromagnetic nuclear decay signatures for neutrino reactions in super-kamiokande*, *Phys. Rev.* **D66** (2002) 013007.
- [51] R. Tomas, D. Semikoz, G. G. Raffelt, M. Kachelriess and A. S. Dighe, *Supernova pointing with low- and high-energy neutrino detectors*, *Phys. Rev.* **D68** (2003) 093013 [[hep-ph/0307050](#)].
- [52] T. Marrodan Undagoitia *et al.*, *Low energy neutrino astronomy with the large liquid scintillation detector lena*, *Prog. Part. Nucl. Phys.* **57** (2006) 283–289 [[hep-ph/0605229](#)].
- [53] M. Wurm *et al.*, *Detection potential for the diffuse supernova neutrino background in the large liquid-scintillator detector LENA*, *Phys. Rev.* **D75** (2007) 023007 [[astro-ph/0701305](#)].
- [54] J. F. Beacom and M. R. Vagins, *Gadzooks! antineutrino spectroscopy with large water cherenkov detectors*, *Phys. Rev. Lett.* **93** (2004) 171101 [[hep-ph/0309300](#)].
- [55] SNAP, letter of intent, <http://snap.lbl.gov/~>.
- [56] <http://www.jwst.nasa.gov/~>.
- [57] H. Yuksel, S. Ando and J. F. Beacom, *Direct measurement of supernova neutrino emission parameters with a gadolinium enhanced Super-Kamiokande detector*, *Phys. Rev.* **C74** (2006) 015803 [[arXiv:astro-ph/0509297](#)].
- [58] T. Iida, “Search for Supernova Relic Neutrinos at Super-Kamiokande”. Talk at the 30th International Cosmic Ray Conference (ICRC), Merida, Yucatan, Mexico. Available at <http://indico.nucleares.unam.mx/confSpeakerIndex.py?confId=4>, 2007.
- [59] C. K. Jung, *Feasibility of a next generation underground water cherenkov detector: Uno*, AIP Conf. Proc. **53** (2000) 29-34; [[hep-ex/0005046](#)].

- [60] K. Nakamura, *Hyper-kamiokande: A next generation water cherenkov detector*, *Int. J. Mod. Phys. A* **18** (2003) 4053–4063.
- [61] L. Mosca, *A european megaton project at frejus*, *Nucl. Phys. Proc. Suppl.* **138** (2005) 203–205.
- [62] D. Autiero *et al.*, *Large underground, liquid based detectors for astro- particle physics in Europe: scientific case and prospects*, *JCAP* **0711** (2007) 011 [arXiv:0705.0116 [hep-ph]].
- [63] A. G. Cocco, A. Ereditato, G. Fiorillo, G. Mangano and V. Pettorino, *Supernova relic neutrinos in liquid argon detectors*, *JCAP* **0412**, 002 (2004) [hep-ph/0408031].
- [64] A. Ereditato and A. Rubbia, *Conceptual design of a scalable multi-kton superconducting magnetized liquid argon tpc*, *Nucl. Phys. Proc. Suppl.* **155** (2006) 233–236 [hep-ph/0510131].
- [65] D. B. Cline, F. Raffaelli and F. Sergiampietri, *Lanndd: A line of liquid argon tpc detectors scalable in mass from 200-tons to 100-ktons*, *JINST* **1** (2006) T09001 [astro-ph/0604548].